Assessment of particle damping device for large laminated structures under acoustic excitations

Nazeer Ahmad[a]1, R Ranganath[a], Ashitava Ghosal[b]

[a]*ISRO Satellite Center, Bangalore 560017, India.*
[b]*Department of Mechanical Engineering, Indian Institute of Science, Bangalore 560012, India.*

Abstract

Solar panels and large reflectors used in spacecraft are made-up of aluminum-honeycomb sandwiched between composite fiber reinforced plastic (CFRP) laminates. Owing to the small inherent damping and large area to mass ratio, such structures are susceptible to strong acoustic excitations during the initial phase of launch. In this paper we present an analytical assessment of the response attenuation of structures equipped with particle dampers. Particle damping is a passive damping technique where the vibration energy of host structure is dissipated by collision of damping particles kept in specially designed cavities in the host structure or in the containers attached to the structure. An existing analytical model, based on the discrete element method (DEM), is used to track the motion of each particle and inter-particle and particle-cavity interactions. The Hertz's dissipative contact model and Coulomb's friction model is incorporated in DEM to model the energy dissipation in normal impacts and tangential components, respectively. The vibration attenuation trend has been studied for location of particle dampers, size of particles, fill fraction and excitation energy. The attenuation has been quantified in terms of power spectral density (PSD) of the vibration responses. The analysis results show significant reduction in PSD for strategically placed particle dampers which could be used advantageously in the design of damping devices for acoustic vulnerable structures.

*Keywords:*Particle impact damping, acoustic, random vibration

Nomenclature

A	area of the panel	p	transient pressure
A_c	area of the coupon	$\boldsymbol{q}$	modal coordinate
$\mathbf{C}$	damping matrix	$\mathbf{R}$	cross-correlation matrix
C_e	equivalent viscous damping	$\boldsymbol{r}$	fill fraction
$\mathbf{D}$	particle damping matrix	$\mathbf{S}$	cross-power spectral density matrix
E_d	energy dissipated	$\mathbf{w}$	transverse displacement
$\boldsymbol{f}^p$	generalized sound pressure force	$\dot{\mathbf{w}}, \ddot{\mathbf{w}}$	velocity and acceleration
$\boldsymbol{f}^d$	generalized particle damping force	ω	excitation frequency
$\boldsymbol{f}^c_{ij}$	Coulomb's friction force	ω_i	natural frequency of plate
H	frequency response function	Φ	modal matrix
h_i	unit impulse response function	α	Hertz's damping constant
$\mathbf{K}$	stiffness matrix	δ	indentation
$\boldsymbol{k}$	generalized stiffness	λ	wave number
K_n	Hertz's stiffness constant	ζ	damping ratio
$\mathbf{M}$	mass matrix	N_c	number contacts
$\boldsymbol{m}$	generalized mass	m_p	mass of the damping particle

1. Introduction

Sandwiched honeycomb composites are used as a base structural element for solar panels and reflectors. They usually have very high area to mass ratio and low inherent damping. Such composites exhibit very large response sunder acoustic excitation which in turn poses danger to the integrity of structure and solar cells mounted on it. It is desired that these excitation be damped and there exists a large amount of literature where

* Corresponding author. Tel.: 080 25083632
E-mail address: nazeer@isac.gov.in

such effort is reported. In this work, we restrict ourselves to particle damping approaches. In particle damping, the damping performance is improved by inserting particle in the empty cells [1, 2] and is also called particle impact damping (PID) or non-obstructive particle damping (NOPD). The PID and NOPD are the passive vibration control techniques wherein the energy of a vibrating system is dissipated by impact and friction. The impact damping technologies usually involve either attaching a container filled with damping particles to a vibrating structure or filling with damping particle a drilled cavity in the host structure [3, 4] at appropriate location. The PID has been successfully used for vibration attenuation in wide range of applications like civil structures against wind and earthquake loads [5], turbine blades, machine tools, space shuttle [6] and aerospace structures [7]. The NOPD is very simple in construction, insensitive to environment, low cost, and effective over wide temperature and frequency range.

The energy dissipation mechanism in PID is highly nonlinear and depends on host of parameters – size, shape, number and material of the particle; enclosure relative geometry and material; mass ratio; volumetric packing fraction; location of PD with respect to structural mode; and level of response. The dissipation of energy takes place mainly through inter-particle and particle-wall impact and friction. The dominant mode of dissipation depends on the relative proportion of different parameters. It is extremely difficult to evolve a model to capture the entire interactions taking place.

The major modelling techniques reported in literature for particle impact damping problem is discrete element method (DEM).The DEM is now an established tool for analysing the dynamic behaviour of assemblies of particles. The DEM is based on Newtonian mechanics where equation of motion of each particle is established by considering the contact forces and moments from the surrounding particle and boundary contacts or from any other source. The motion of each particle and its interaction with surrounding boundaries is tracked. For the larger problems where millions of particle motion is required to be solved coupled with the dynamics of the structure, the DEM becomes frustratingly inefficient. In this paper large amount of particles are required to affect the structural response as the dimensions of the panel runs in meter. Therefore in this work DEM is applied on a coupon of smaller size and same composite material and damping particle. The coupon is subjected to vibration loads and the energy dissipated is estimated and further its dependence on the other parameter is studied. The honeycomb cells are small in dimensions and the number parameters is reduced. An equivalent damping constant of viscous damper which dissipates same amount of energy per cycle is estimated and incorporated in the equations of motion of plate.

2. Mathematical formulations

The finite element equations of motion of a plate representing a typical solar panel with particle damping in acoustic field can be written as:

$$\mathbf{M}\ddot{\mathbf{w}} + \mathbf{C}\dot{\mathbf{w}} + \mathbf{K}\mathbf{w} = \mathbf{f}^{\mathbf{p}} - \mathbf{f}^{\mathbf{d}} \tag{1}$$

where the force vector , $\mathbf{f}^{\mathbf{p}}$, is due to transient pressure acting on the exposed area due to sound field. It can expressed as

$$\mathbf{f}^{\mathbf{p}} = P(t)\mathbf{A} \tag{2}$$

where the diagonal matrix $\mathbf{A}$ is the projected matrix on nodes of the FEM, and $\mathbf{f}^{\mathbf{d}}$ is the equivalent force due to particle damping. The honeycomb sandwiched coupon of the size 5cm x 5cm filled with acrylic particle is subjected to harmonic motion in the range of 5 to 2 kHz in steps of 10Hz and the energy dissipated is calculated using the Eq.(3). The details of the DEM used for calculating the particle motion and its interaction with the walls of the cells can be found in references [8-10]. The energy dissipated is made up of the normal impact and Coulomb's friction and can be written as

$$E_d = \frac{\sum_{k=1}^{N_c} \int_0^{t_c} \left(\alpha \sqrt{m_p k_n}\, \delta^{1/4} \dot{\delta}_{ij} \dot{\delta}_{ij} + F_{ij}^{c} \dot{\delta}_{ij} dt \right) dt}{A_c} \tag{3}$$

The energy dissipated per cycle per unit area can be equated to the energy dissipated by viscous damper with equivalent damping C_e as

$$E_d = \int_0^{2\pi/\omega} C_e \dot{w} dt \tag{4}$$

A parametric study of variation of E_d with respect to the parameters of the DEM such as filling fraction, excitation frequency, and displacement amplitude suggests that the energy dissipated is mainly a dependent on filling fraction and excitation frequency. Similar results are also reported in the experimental work of [1]. Integrating Eq. (4) and using similar interpolation equation as is given in reference [1] for E_d, equivalent damping can be written as

$$C_e = \frac{1}{2\pi} a_1 \omega^{a_2 - 1} e^{-a_3 \omega} \tag{5}$$

The constant are given as

$$\begin{aligned} a_1 &= r(-20 + 36.09r - 25.2r^2)10^{-4} \\ a_2 &= 4.10 - 0.6r \\ a_3 &= r(8.8 - 12.5r)10^{-4} \end{aligned} \tag{6}$$

The equivalent damping force acting on the FEM element covering the area filled with damping particles can be obtained as

$$\begin{aligned} \mathbf{f_e^d} &= -\int_{A_e} C_e \dot{\mathbf{w}} dA = -C_e \int_{A_e} \mathbf{N_{wi}} \mathbf{N_w^T} \dot{\mathbf{w}} dA = -C_e \mathbf{D_e} \dot{\mathbf{w}} \\ \mathbf{D_e} &= \int_{A_e} \mathbf{N_{wi}} \mathbf{N_w^T} dA \end{aligned} \tag{7}$$

where $\mathbf{D_e}$ is the damping matrix. The Eq. (1) can be recast in modal space by linear transformation of co-ordinates, $\boldsymbol{w} = \boldsymbol{\Phi q}$, where the modal matrix $\boldsymbol{\Phi} = \begin{bmatrix} \phi_1 & \cdots & \phi_n \end{bmatrix}$ consists of the column vectors of normal modes.Invoking the mass and stiffness orthogonality conditions: $\text{diag}\left[\boldsymbol{\Phi}^T \mathbf{M} \boldsymbol{\Phi}\right] = \mathbf{m}$ and $\text{diag}\left[\boldsymbol{\Phi}^T \mathbf{K} \boldsymbol{\Phi}\right] = \mathbf{k}$, where $\mathbf{m}$ and $\mathbf{k}$ are the generalized mass and stiffness matrices, Eq. (1) can be written as:

$$\ddot{\mathbf{q}}_\mathbf{i} + 2\zeta \boldsymbol{\omega}_\mathbf{i} \dot{\mathbf{q}}_\mathbf{i} + \boldsymbol{\omega}_\mathbf{i}^2 \mathbf{q}_\mathbf{i} = \frac{\boldsymbol{\phi}_\mathbf{i}^\mathbf{T}}{\mathbf{m_i}} \left(\mathbf{f_i^p} + \mathbf{f_i^d} \right) \qquad i = 1,2,...,n \tag{8}$$

Inserting Eq. (7) in Eq. (8) we get

$$\ddot{\mathbf{q}}_\mathbf{i} + 2\zeta \boldsymbol{\omega}_\mathbf{i} \dot{\mathbf{q}}_\mathbf{i} + \boldsymbol{\omega}_\mathbf{i}^2 \mathbf{q}_\mathbf{i} = \frac{\boldsymbol{\phi}_\mathbf{i}^\mathbf{T}}{\mathbf{m_i}} \mathbf{f_i^p} - \frac{\mathbf{C_e}}{\mathbf{m_i}} \mathbf{D_i} \dot{\mathbf{q}}_\mathbf{i} \qquad i = 1,2,...,n \tag{9}$$

where

$$\mathbf{D_i} = \left[\boldsymbol{\Phi}^\mathbf{T} \mathbf{D} \boldsymbol{\Phi} \right]_i \tag{10}$$

Rearranging the Eq. (9) we get

$$\ddot{\mathbf{q}}_\mathbf{i} + \left(2\zeta \boldsymbol{\omega}_\mathbf{i} + \frac{C_e}{\mathbf{m_i}} \mathbf{D_i} \right) \dot{\mathbf{q}}_\mathbf{i} + \boldsymbol{\omega}_\mathbf{i}^2 \mathbf{q}_\mathbf{i} = \frac{\boldsymbol{\phi}_\mathbf{i}^\mathbf{T}}{\mathbf{m_i}} \mathbf{f_i^p} = \mathbf{F_i^p}; \qquad i = 1,2,...,n \tag{11}$$

Now taking Laplace transform of the above equation, we have

$$\left(s^2 + 2s\left(\zeta\omega_i + \frac{C_e}{2\mathbf{m}_i}\mathbf{D_i} \right) + \omega_i^2 \right)\mathbf{q_i}(s) = \mathbf{F_i^p}(s); \qquad i = 1,2,...,n \tag{12}$$

The time domain response and unit impulse response of the above equation is given as:

$$\mathbf{q_i} = \int_0^t h_i \mathbf{F_i^p}(t-\tau)d\tau \qquad i = 1,2,...,n \tag{13}$$

where unit impulse response h_i is given as:

$$\begin{aligned} h_i &= e^{-\left(\zeta\omega_i + \frac{C_e}{2\mathbf{m}_i}\mathbf{D_i}\mathbf{f_i^d}\right)} \frac{\sin(\omega_d t)}{\omega_d}, \qquad i = 1,2,...,n \\ \omega_d &= \omega_i \left[1 - \zeta^2 - \left(\frac{C_e}{2\mathbf{m_i}}\mathbf{D_i} \right)^2 - \zeta \frac{C_e}{\mathbf{m_i}}\mathbf{D_i} \right]^{1/2} \end{aligned} \tag{14}$$

The modal frequency response function is given as:

$$H_i(\omega) = \frac{\omega_i^2}{\left(\omega_i^2 - \omega^2\right) + 2j\omega\left(\zeta\omega_i + \frac{C_e}{2\mathbf{m_i}}\mathbf{D_i} \right)} \qquad i = 1,2,...,n \tag{15}$$

and the cross correlation function and PSD of the modal coordinates and can be obtained as:

$$\mathbf{R_{q_i q_j}} = \lim_{T\to\infty} \frac{1}{2T} \int_{-T}^{T} \mathbf{q_i}(t)\mathbf{q_j}(t-\tau)d\tau; \quad \mathbf{S_{q_i q_j}} = \int_{-\infty}^{\infty} \mathbf{R_{q_i q_j}}(\tau)e^{-j\omega t}d\tau \qquad i,j = 1,2,...,n \tag{16}$$

Likewise the correlation function of the generalized force vector of sound field can be written as:

$$\mathbf{R_{f_i^p f_j^p}} = \lim_{T\to\infty} \frac{1}{2T} \int_{-T}^{T} \mathbf{f}_i^p(t)\mathbf{f}_j^p(t-\tau)d\tau; \qquad i,j = 1,2,...,n \tag{17}$$

$$\mathbf{R}_{f_i^p f_j^p}(\tau) = \lim_{T\to\infty} \frac{1}{2T} \int_{-T}^{T} \frac{\boldsymbol{\phi}_i^{\mathsf{T}} \mathbf{A}_i \mathbf{f}_i^p(t)\mathbf{f}_j^p(t-\tau)\mathbf{A}_i\boldsymbol{\phi}_j}{\mathbf{m_i m_j}} d\tau; \qquad i,j = 1,2,...,n \tag{18}$$

where A_i is the i[th] column of matrix A. It may be noted that Eq. (18) relates the generalized force cross-correlation to the acoustic pressure fields as cross- correlation matrix.

$$\mathbf{R}_{f_i^p f_j^p}(\tau) = \frac{\boldsymbol{\phi}_i^T \mathbf{A}_i \mathbf{R}_{p_i p_j} \mathbf{A}_j \boldsymbol{\phi}_j}{\mathbf{m_i m_j}}; \qquad i,j = 1,2,...,n \tag{19}$$

and the cross-power spectral densities are given as

$$\mathbf{S}_{f_i^p f_j^p} = \frac{\boldsymbol{\phi}_i^T \mathbf{A}_{p_i} \mathbf{S}_{p_i p_j} \mathbf{A}_{p_j} \boldsymbol{\phi}_j}{\mathbf{m}_i \mathbf{m}_j}; \qquad i,j = 1,2,...,n \tag{20}$$

The matrix of cross-power spectral densities of the pressure $\mathbf{S}_{P_iP_j}$ is expressed as the product of references PSD of sound pressure level (SPL) and a coherence function matrix which relates the pressure at different points in the sound field given as.

$$\mathbf{S}_{p_i p_j} = S_p(\omega)\ \mathbf{C}_{p_i p_j}(\omega) \tag{21}$$

A reverberant field can be expressed by a coherence function [11] as.

$$\mathbf{C}_{p_i p_j}(\omega, \mathbf{r_i}, \mathbf{r_j}) = \frac{\sin(k\left|\mathbf{r_i} - \mathbf{r_j}\right|)}{k\left|\mathbf{r_i} - \mathbf{r_j}\right|} \tag{22}$$

where k is the wave number and $\mathbf{r}_i, \mathbf{r}_j$ are the position vectors of two points. In this work we are interested in computing the auto PSD at the points of interests only and Eq. (22) can be replaced by a unit matrix.
The cross-PSD of the modal coordinates can be written using Eq. (13) as:

$$\mathbf{S}_{q_i q_j} = \int_{-\infty}^{\infty} \lim_{T\to\infty} \frac{1}{2T} \left(\int_{-T}^{t} \left(\int_{-\infty}^{\infty} h_i(\alpha) f_i(t-\alpha) d\alpha \right) \left(\int_{-\infty}^{\infty} h_j(\beta-\tau) f_j(t-(\beta-\tau))\beta \right) \right) e^{-j\omega\tau} d\tau dt \tag{24}$$

After some algebraic manipulation, Eq. (24) can be written as:

$$\mathbf{S}_{q_i q_j} = \frac{\mathbf{H}_i(\omega)\phi_i^T \mathbf{A}\mathbf{S}_{p_i p_j} \mathbf{A}\phi_i \mathbf{H}_i^*(\omega)}{\omega_i^2 \omega_j^2 m_i m_j} \tag{25}$$

and finally the cross-power spectral density of acceleration is related to the cross power spectral density of the modal coordinate as:

$$\mathbf{S}_{\ddot{w}_i \ddot{w}_j} = \omega^4 \Phi \mathbf{S}_{q_i q_j} \Phi^T \tag{25}$$

3. Results and discussions

Numerical simulations were carried on a rectangular aluminum honeycomb sandwiched composite of dimensions 1.5m x 1m x 0.025m. The panel is divided into 600 hundred finite elements. areas of 20 cm x 20 cm of the honeycomb is considered for filling with damping particles and named PID-1, PID-2 and PID-3 as shown in Fig. (2). the area of a single patch is 0.0267 times that of the panel. Low density damping particles like acrylic is considered as filling particle so as not to change the mass and dynamics of the panel significantly.

The PSD responses at points 326, 189 and 318 of the FEM grid are considered for assessing the effect of PID. These locations are chosen so that the most of the plate modes responds at these locations.

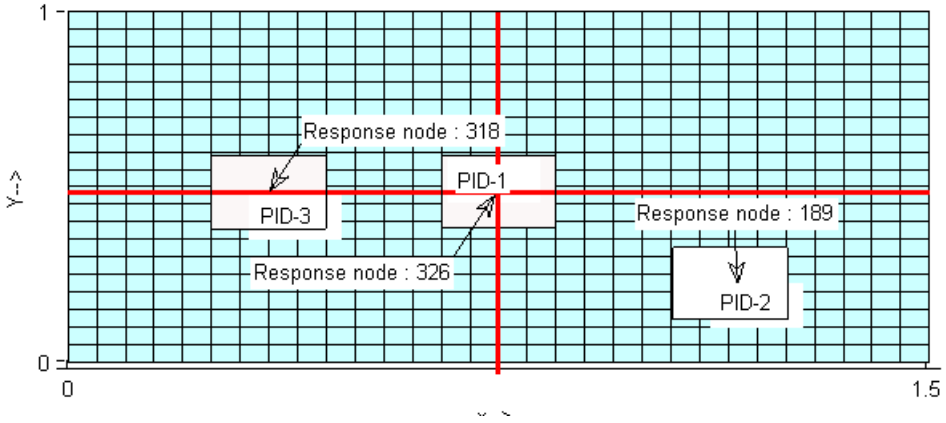

Fig. 1: Locations of PID, response points on FEM grid

The frequencies and modal orders which decides the mode shape of the plate considered in the simulation is given in Table-1

Table 1. Modal frequency and mode order

m	n	Frequency
1	1	64.90
2	1	124.81
1	2	199.70
3	1	224.67
2	2	259.62
3	2	359.46
1	3	424.37
2	3	484.28
3	3	584.13
1	4	738.90
4	2	499.26
4	3	723.92
2	4	798.81
4	4	1038.46
6	3	1123.33
6	4	1437.87
7	2	1158.28
7	4	1697.48
8	1	1323.04
5	1	544.19
7	1	1023.48
9	1	1662.53

3.1. Effect of fill fraction

The effect of fill fraction on PSD response at selected grid points is studied for PID-1 which is at the centre of the simply supported panel. The panel is excited by an acoustic field described by its SPLin Fig. 2. The SPL represented on 1/3 octave centre frequency is typical level of acoustic field that exits at during the launch of spacecraft.

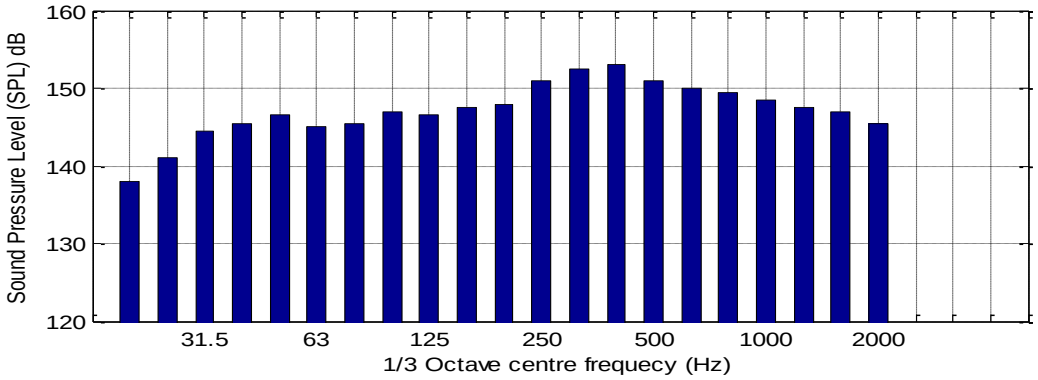

Fig. 2: The input SPL

The acceleration PSD response monitored at grid points: 326,189 and 318 is plotted in Figs.3-5. The PSD responses are decreasing at resonances at all three locations. At all location a fill fraction of 10% is seen to be most effective. The effect of particle impact damping is more prominent in higher frequency range as compared to low frequency. The response at node (326) that is on the damper and centre of the panel is decreasing for all fill fractions as shown in Fig. (3). However the responses at all the locations increases as fill fraction is change from 10%. The responses are almost same for fill fractions from 70 to 90.

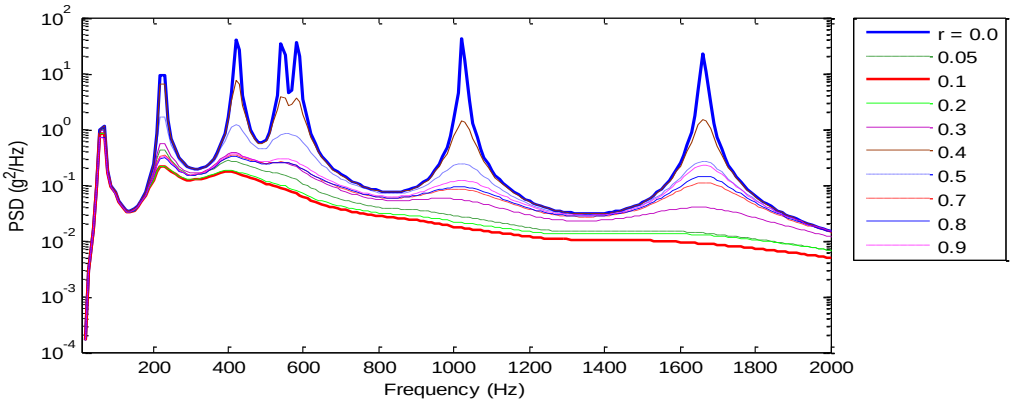

Fig.3 Acceleration PSD response of grid point 326

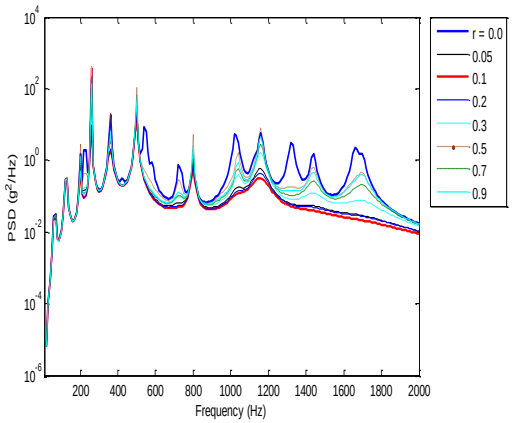

Fig.4 Acceleration PSD response of grid point 189

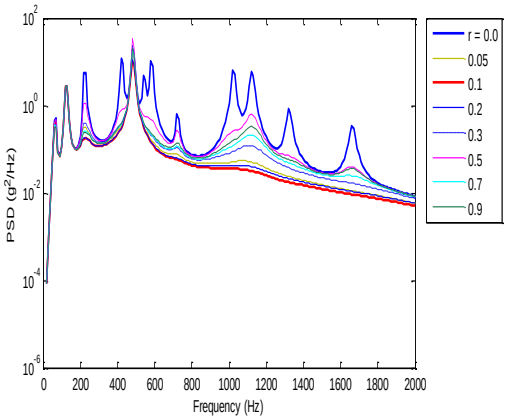

Fig.5 Acceleration PSD response of grid point 318

3.2. Effect of location

To study the effect of location of the damper, the panel is excited by the same SPL as given in Fig. 2 and constant fill fraction of 50% with one of the PID active at a time. The response at the node near to the damper is less as compared to the farther one.Similar behavior is seen for all three dampers. Figs 6-7 present the PSD responses at nodes 189 and 326, respectively, when damper position is change from location 1 to 3

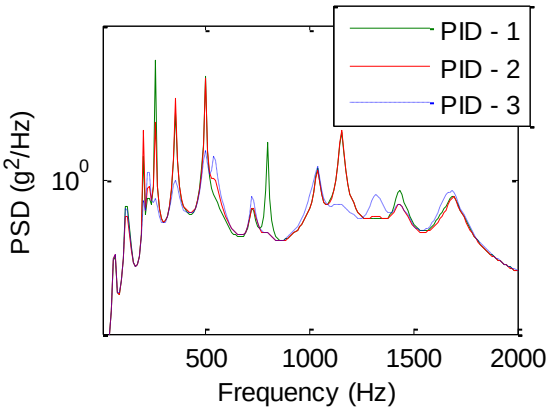

Fig.6 Acceleration PSD response of grid point 189

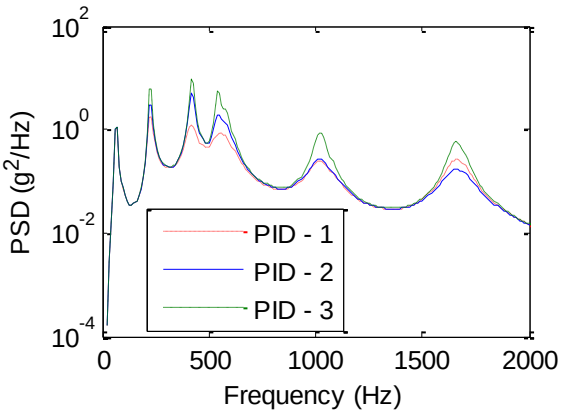

Fig.7 Acceleration PSD response of grid point 326

3.3. Effect of excitation level

The response behaviour of the panel is studied for 3 excitation levels: 162 dB, 152dB and 142dB overall SPL. The spectrum corresponding to 162 dB shown in Fig.2 is scaled down in steps of 10dB uniformly in all frequency bands to get other input levels. The acceleration response is seen to be shifting linearly on logarithmic scale as shown in Figs.8. Such response is expected from the Eq.(21) and Eq.(25).

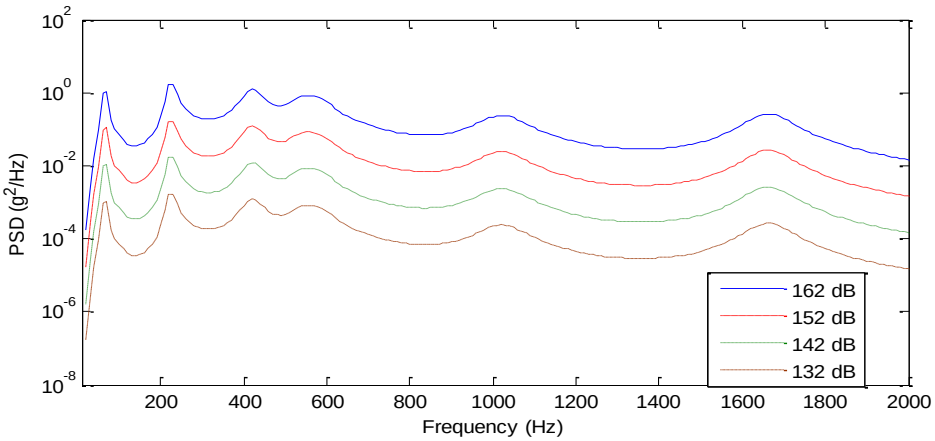

Fig.8 Acceleration PSD response of grid point 326

Conclusions

Study of acceleration response of large honeycomb composite structures used in spacecraft treated with impact-damping-particle under acoustic excitations is carried out. An equivalent damping model for particle damping device was arrived from coupon level test was used to study the response of the panel with respect to parameters of the damping device. The performance of the device was found to depending on the fill fraction, location of device and excitation level. The panel response was seen to be lowest at smaller fill fraction. However the trend was not monotones. The response was seen less near the device compared to faraway locations and with respect to excitation level it was linearly increasing in all frequency bands.

Acknowledgements

The first author is grateful to Dr. K. Renji, GD, Structures, and S. Shankar Narayan, Division Head, Dynamics Testing for their cooperation and encouragements.

References

[1] J. G. Michon, A. Almajid, G. Aridon, Soft hollow particle damping identification inhoneycomb structures, Journal of Sound and Vibration 332 (3) (2013) 536-544.
[2] WB. Wang, M. Yang, Damping of honeycomb sandwich beams, Journal of MaterialsProcessing Technology 105 (1-2) (2000) 67-72.
[3] Z. Xu, M. Y. Wang, T. Chen. An Experimental Study of Particle Damping forBeams and Plates, Journal of Vibration and Acoustics.126 (1)(2004) 141.
[4] Z. Xu, M. Y. Wang, T. Chen, Particle damping for passive vibration suppression:Numerical modelling and experimental investigation, Journal of Sound and Vibration 279 (3-5) (2005) 1097-1120.
[5] G.Z. Lu, X. Lu, W. Lu, S. F. Masri, Experimental studies of the efects of buferedparticle dampers attached to a multi-degree-of-freedom system under dynamic loads,Journal of Sound and Vibration 331 (9) (2012) 2007-2022.
[6] J. J. Moore, A. B. Palazzolo, R. Gadangi, T. A. Nale, S. A. Klusman, G. V. Brown,A. F. Kascak, A Forced Response Analysis and Application of Impact Dampersto Rotordynamic Vibration Suppression in a Cryogenic Environment, Journal ofVibration and Acoustics 117 (3A) (1995) 300-310.
[7] B. Knight, D. Parsons, A. Smith, Evaluating Attenuation of Vibration Responseusing Particle Impact Damping for a Range of Equipment Assemblies, in: AIAAAerospace Design and Structures Event; 8-11 Apr. 2013; Boston, MA; United States,1-9, 2013.
[8] M. Saeki, Analytical study of multi-particle damping, Journal of Sound and Vibration 281 (3-5) (2005) 1133-1144.
[9] M. Saeki, Impact Damping with Granular Materials in a Horizontally VibratingSystem, Journal of Sound and Vibration. 251 (1) (2002)153-161.
[10] X. Fang, J. Tang, H. Luo, Granular damping analysis using an improved discreteelement approach, Journal of Sound and Vibration 308 (1-2) (2007) 112-131.
[11] Richard K Cook, R. V. Waterhouse,R.D. Berendt,Seymour Edelman, M.C. Thompson Jr., Measurement of correlation coefficients in reverberant sound fields. Journal of Acoustics Society America, Vol. 27,Page.1072 (1955)